SUPPLEMENTARY INFORMATION

Novel single pass biogas-to-diesel process using a Fischer-Tropsch catalyst designed for high conversion

Table S-1: Stream table for the syngas generation system for the base case scenario (Fischer-Tropsch synthesis operating at X_{CO}=60% using a Pt-Co/Al_2O_3-catalyst including a hydrocracking unit; stream numbers refer to Aspen model given in Figure 3).

Stream	***1***	***3***	***7***	***8***	***9***	***11***	***12***	***24***	***22***
Stream	**Biogas feed**	**Water feed**	**Tri-reformer feed**	**Tri-reformer product**	**Water addition to WGS**	**WGS feed**	**WGS product**	**Syngas product**	**H_2 product**
T (°C)	25	25	220	750	25	280	300	220	50
P (bar)	1	1	2.7	2.7	2.7	2.7	2.7	20	10
	Molar flow rate (kmol/hr)								
CO_2	100	0	100	125	0	125	144	141	2.5
CH_4	300	0	300	9.07	0	9.07	9.07	9.07	0.00
CO	0	0	0	266	0	266	247	247	0.31
H_2O	0	140	120	184	20	204	185	11.7	0
O_2	190	0	190	0	0	0	0	0	0
H_2	0	0	0	518	0	518	537	501	36.3
N_2	714	0	714	714	0	714	714	714	0.38

Table S-2: Stream table for the separation and refining section for the base case scenario (Fischer-Tropsch synthesis operating at X_{CO}=60% using a Pt-Co/Al_2O_3-catalyst including a hydrocracking unit; stream numbers refer to Aspen model given in Figure 5)

Stream	***24***	***25***	***29***	***30***	***32***	***35***	***36***	***44***	***46***	***47***	***49***	***50***
Description	**FT product**	**FT product vapour**	**Cold cond. vapour**	**Cold cond. liquid**	**Pressurized tail gas**	**Water knock out liquid**	**FT product liquid**	**Hydrocrack. product**	**Atm. dist. Feed**	**Tail gas**	**Distillate**	**Wax**
P (bar)	19	19	19	19	19	19	19	34	1.1	1	1	1
T (°C)	20	220	50	50	35	35	220	370	180	150	300	356
	Molar flow rate (kmol/hr)											
CO_2	143	143	143	0.2	143	0.0	0.0	0.0	0.2	0.2	0.0	0.0
CH_4	21	21	21	0.0	21.3	0.0	0.0	2.5	2.5	2.5	0.0	0.0
CO	99	99	99	0.0	99	0.0	0.0	0.0	0.0	0.0	0.0	0.0
H_2O	156	156	26	3.8	15.2	137	0.0	0.0	3.8	3.8	0.0	0.0
H_2	210	210	210	0.0	210	0.0	0.0	0.0	0.0	0.0	0.0	0.0
N_2	714	714	713	0.1	713	0.0	0.0	0.0	0.1	0.1	0.0	0.0
C_2-C_4	2.3	2.3	2.3	0.0	2.3	0.0	0.0	0.3	0.3	0.3	0.0	0.0
C_5-C_9	3.4	3.4	2.4	1.0	2.4	0.0	0.0	1.4	2.4	2.3	0.1	0.0
C_{10}-C_{22}	3.9	3.3	0.1	3.2	0.1	0.0	0.6	1.9	5.0	0.7	3.7	0.6
C_{22+}	1.6	0.2	0.0	0.3	0.0	0.0	1.4	0.4	0.7	0.0	0.1	0.6

Table S-3: Stream table for the combined cycle power plant for the base case scenario (Fischer-Tropsch synthesis operating at X_{CO}=60% using a Pt-Co/Al_2O_3-catalyst including a hydrocracking unit; stream numbers refer to Aspen model given in Figure 6)

Stream	***32***	***47***	***52***	***53***	***54***	***55***	***56***	***58***	***59***	***61***
Stream	**Pressurized tail gas**	**Tail gas**	**Gas turbine product**	**Air feed**	**Combined tail gas**	**Combustion unit product**	**Water feed**	**Boiler steam**	**Steam turbine product**	**Boiler flue gas**
T (°C)	35	150	137	35	140	1278	27	620	102	650
P (bar)	19	1	1	1.1	1	1	100	100	1.1	1
					Molar flow rate (kmol/hr)					
CO_2	143	0.2	143	0	143	314	0	0	0	314
CH_4	21	2.5	21	0	23.5	0	0	0	0	0
CO	99	0.0	99	0	99	0.02	0	0	0	0.02
H_2O	15.2	3.8	15.2	0	19	326	1074	1074	1074	326
O_2	0	0	0	400	0	128	0	0	0	128
H_2	210	0	210	0	210	0.01	0	0	0	0.01
N_2	713	0.1	713	1504	713	2217	0	0	0	2217
C_2-C_4	2.3	0.3	2.3	0	2.6	0	0	0	0	0
C_5-C_9	2.4	2.3	2.4	0	4.7	0	0	0	0	0
C_{10}-C_{22}	0.1	0.7	0.1	0	0.8	0	0	0	0	0
C_{22+}	0.0	0.0	0.0	0	0	0	0	0	0	0

Table S-4: Exponential constants ($a \cdot e^{b \cdot x}+c$) for the empirical modelling of selectivity data of Pt-Co/Al_2O_3 and Mn-Pt-Co/Al_2O_3

		C_{5+} Selectivity	**CH_4 selectivity**	**Chain growth probability**	**CO_2 selectivity**
Pt-Co/Al_2O_3	a	-0.02	0.000077	-0.000066	0.0017
	b	0.08	0.13	0.08	0.10
	c	91	8.0	0.92	0.59
Mn-Pt-Co/Al_2O_3 (Mn:Co = 0.15)	a	-0.00016	0.000000016	-0.0001	0.0000059
	b	0.12	0.22	0.08	0.14
	c	95	4.56	0.90	0.40

Table S-5: Regional diesel specifications for the US, EU, Africa and South Africa

	Diesel specifications				
	ASTM D975: 15b (US)	**EN 590:2014 (EU)**	**EN 15940:2016 (EU)**	**AFRI-5 2016 (AU)**	**SANS 342:2016 (ZA)**
Diesel density at 15°C	-^{a}	820	765-800	820-880	805-850
Sulphur, ppm	<15	<10.0	<5.9	50	10^{b}
Polycyclic aromatic hydrocarbons (max mass %)	- ^{a}	- ^{a}	8	- ^{a}	8
Water, ppm	500	200	< 200	- ^{a}	250
Cetane number min	49	51	70	49	51
Viscosity at 40°C mm²/s	1.9 - 4.1	2.0 - 4.5	2.0-4.5	-^{a}	2.2-5.3
Flash Point, °C	55	55	55	-^{a}	
Cloud Point, °C					
Winter	-5 to - 34	-10 to -34	-10 to -34	-^{a}	+6
Summer					-^{a}
Distillation					
T_{95}	370	360	360	-^{a}	362
T_{90}	338				360
	[52]	[52]	[52,56]	[53]	[54]

^{a} No limit specified

^{b} Based on low sulphur diesel. Standard diesel is rated at 500 mg/kg.

Tri-reformer

The choice of feed composition (oxygen- and steam-to-carbon ratios) and reactor temperature affect the product composition, yields and conversions of the tri-reformer. For the context of small-scale decentralized applications, it was critical that the tri-reformer operate adiabatically. Thus, the feed needed enough oxygen to enhance the exothermic combustion reaction.

Figure S-1 illustrates the effect of the steam-to-carbon (S/C) ratio and temperature on the conversion of CH_4 and CO_2, the CO and H_2 yield and the H_2/CO ratio for an adiabatic tri-reformer with an air feed adjusted to ensure a net duty of zero.

The CH_4 conversion (Figure S-1 (a)) increased rapidly with increasing temperature. At 500°C, X_{CH_4} lay between 20% and 40% whilst at temperatures above 800°C, X_{CH_4} was close to 100%. Unfortunately, in order to reach these high temperatures, more oxygen was required, and thus air, which increased the diluent factor for the Fischer-Tropsch synthesis. An increase in the steam-to-carbon (S/C) ratio further increased the conversion, with a noticeable effect at temperatures below 800°C.

Unfortunately, whilst a high CH_4 conversion is likely, a high conversion of CO_2 is less likely (Figure S-1 (b)), due to the combustion and water-gas shift reactions. Mostly negative conversions were found throughout the temperature range, with the exception of a steam-to-carbon ratio of 0 at high temperatures [57]. Operating with oxygen but no steam (oxy-CO_2 reforming) is not feasible due to safety concerns [28]. Increasing in the steam-to-carbon ratio above 0 unfortunately decreased the CO_2 conversion significantly.

Figures S-1 (c) and (d) show the effect of temperature and steam-to-carbon ratio on the yield of H_2 (H-%) and CO respectively (C-%). Hydrogen yield was defined as the amount of hydrogen produced, considering the amount of atomic hydrogen contained in feed CH_4 and H_2O. CO yield was defined as the carbon yield from CO_2 and CH_4. Increasing temperatures favored higher yields of CO and H_2, although the H_2 yield reached a maximum between 700°C and 800°C. Increasing steam-to-carbon ratio and temperature at low temperatures increased the H_2 yield, however this trend reversed at high temperatures, which may be due to contributions from the reverse water-gas shift reaction. Increasing the steam-to-carbon ratio decreased the CO yield across the entire range of temperature, with a more significant effect at 750°C.

Figure S-1 (e) shows the effect of the steam-to-carbon ratio and the reformer temperature on the syngas (CO and H_2) partial pressure exiting the tri-reformer. The syngas partial pressure increased with increasing temperature until a point between 700ºC and 850ºC (depending on the steam-to-carbon ratio), after which it started to decrease. The increase in syngas partial pressure between ca. 500ºC and 700ºC can be attributed to the increase in CO and H_2 yield with increasing temperatures in the same range.

The decrease in the syngas partial pressure above ca. 700ºC can be attributed to the decrease in the H_2 yield at a similar point, as well as the influence of the increasing concentration of inert N_2 (since more air is required for adiabatic operation with increasing temperatures). Increasing the steam-to-carbon ratio improved the partial pressure of syngas in the tri-reformer product at low temperatures and decreased it at high temperatures. This is like the trend for H_2 yield.

An increase in temperature had a strong negative effect on the H_2/CO ratio (Figure S-1 (f)) for all steam-to-carbon ratios. At a S/C = 0.4, a temperature increases from 500ºC to 700ºC decreased the H_2/CO ratio from 5.5 to 2.2. Above 700°C the effect of temperature had a weaker effect. At a S/C = 0.4, an increase in temperature from 700°C to 900°C resulted in a decrease from 2.2 to 1.8. Increasing the S/C improved the H_2/CO ratio significantly, especially at low temperatures. Interestingly, this data suggests that at temperatures as low at 750ºC, a S/C ratio of less than 0.3 may be used to achieve a H_2/CO ratio appropriate for the Fischer-Tropsch synthesis.

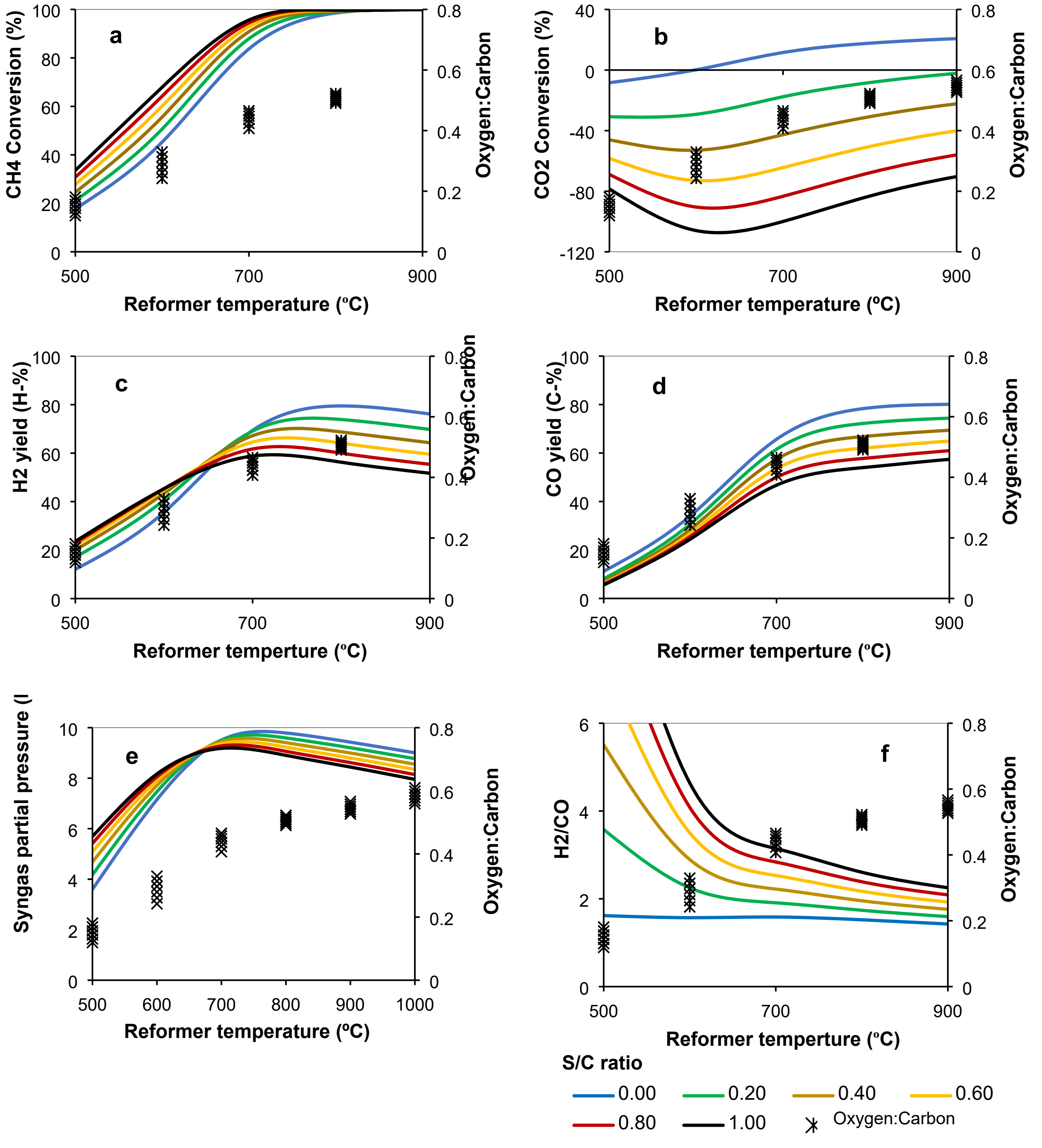

Figure S-1: The effect of temperature and steam-to-carbon ratio on the (a) CH_4 conversion, (b) CO_2 conversion, (c) H_2 yield, (d) CO yield and (e) syngas partial pressure and (e) product H_2:CO ratio for autothermal tri-reforming. The oxygen-to-carbon ratio required to maintain autothermal conditions, at different steam-to-carbon ratios is shown on the secondary axis.

Water-gas shift reactor

Figure S-2 shows the sensitivity analysis for the water-gas shift reactor, including the change in exit H_2/CO ratio with (a) additional steam addition (S/C ratio) and (b) catalyst weight, at different feed temperatures, for a feed consistent with the base case for the product of a tri-reformer operating adiabatically at 750°C with a S/C ratio of 0.3 and an O_2/C ratio of 0.475. The additional S/C ratio in the x-axis of Figure S-2 refers to the water entering the WGS unit from Stream 9, rather than the water left over after the tri-reformer. Figure S-2 (a) is calculated for a catalyst weight of 0.03 kg whilst Figure S-2 (b) is calculated for an additional steam-to-carbon ratio of 0.2.

Increasing the water-gas shift temperature and additional S/C ratio increased the exit H_2/CO ratio to varying extents (Figure S-2 (a)). Without any additional water, the H_2/CO ratio could be shifted from under 2 to 2.3 by increasing the inlet temperature from 210°C to 310°C due to an enhanced rate of reaction per gram catalyst (Equation 1). As the temperature in the water-gas shift unit is controlled by a cooler after the tri-reformer, the exit H_2/CO ratio could be controlled by the coolant flow rate without the need for excess water addition. This is a benefit as it decreases the requirements of the water-knock out pots and compressors downstream.

Figure S-2 (a) further shows that increasing the S/C ratio increased the H_2:CO ratio with a more significant effect at higher temperatures. Luckily, in order to satisfy the requirements of the hydrocracker, even at extremely high H_2:HC ratios (4000 m_n^3/m^3), a H_2/CO ratio of less than 2.4 is required. Thus, the inlet temperature need not be increased above 310ºC.

Figure S-2 (b) shows the change in H_2:CO ratio with increasing catalyst (Pt/TiO_2) weight for an additional S/C ratio of 0.2. Increasing the catalyst weight between 0 to 0.04 kg increased the exit H_2:CO ratio, with larger gradients at higher temperatures. A catalyst weight between 0.03 and 0.04 kg would easily be able to meet the requirements of this process (H_2:CO ratio between 2 and 2.4).

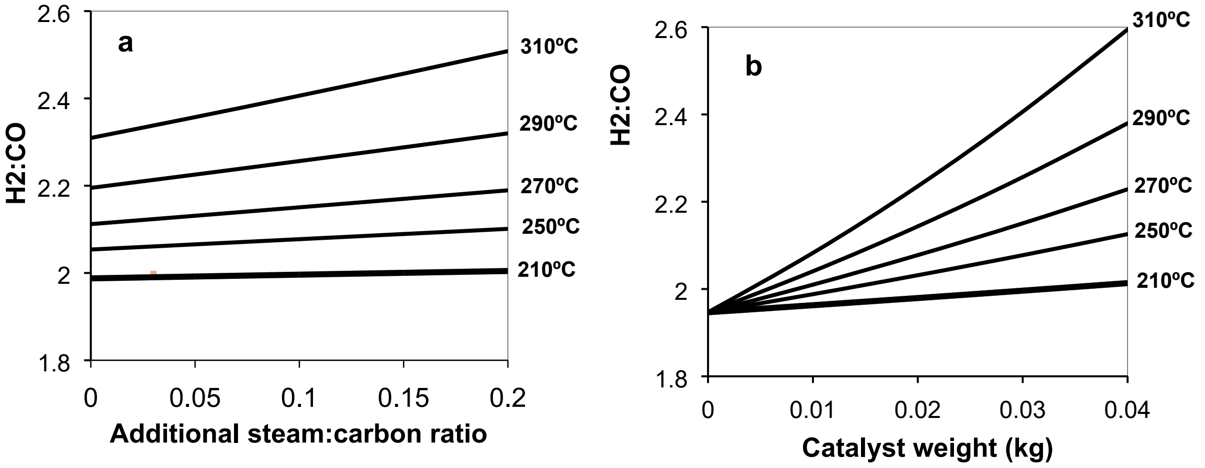

Figure S-2: Sensitivity analysis of the water gas shift reactor showing the change in exit H_2/CO ratio with (a) extra steam addition for 0.03 kg of catalyst and (b) catalyst weight at an additional S/C ratio of 0.2. Feed and inlet conditions as presented in the base case stream table.

Optimal conditions for tri-reformer / water-gas shift

Choosing optimal conditions for the tri-reformer requires the balancing of two objectives: optimizing the carbon yield and ensuring that the desired H_2:CO ratio is attained after the water-gas shift unit. In theory, this appears to be a simple task of optimizing the carbon yield of the tri-reformer (low steam-to-carbon ratio and a high temperature) and using the water-gas shift reactor to adjust the H_2:CO ratio (which decreases with temperature). However, as the water-gas shift unit converts CO into CO_2, the carbon yield decreases significantly in this step.

Figure S-3 shows the CO yield of the reformer product and the water-gas shift product for the case where an H_2:CO ratio of 2 (no hydrocracking) and 2.4 (hydrocracking with extremely high H_2: HC ratio) is required. This analysis is based on a reformer (at a range of temperatures) operating adiabatically with a S/C ratio of 0.3 and an O_2/C ratio of 0.475. The water-gas shift is operating at 280°C with an additional S/C ratio of 0.2. The catalyst weight in the water-gas shift reactor is increased from 0.01 to 0.1 in each case such that the desired H_2:CO ratio (2 or 2.4) may be attained. Figure S-3 also shows the corresponding H_2:CO ratios for each case (in red).

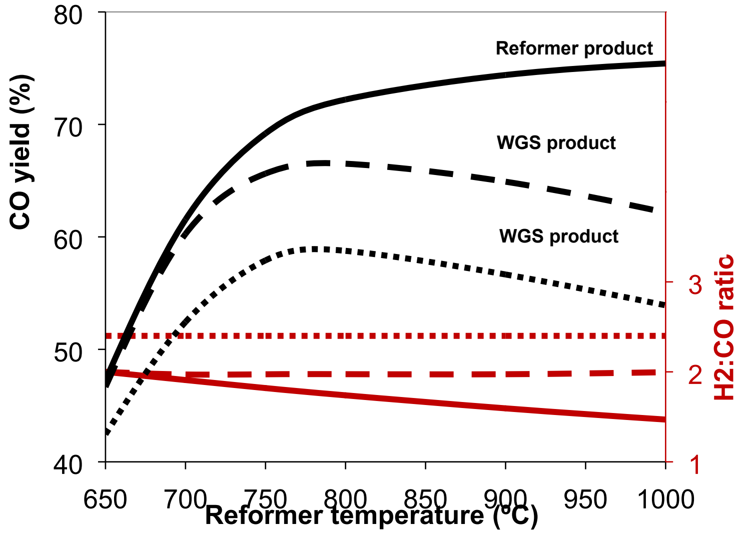

Figure S-3: The CO yield (●) and H_2:CO ratio (●) for the reformer product (▔▔) and the water-gas shift product after shifting the H_2:CO ratio to 2 (---) and 2.4 (···) for various reformer temperatures. Reformer S/C ratio = 0.3 and O_2/C ratio = 0.475. Water gas shift S/C ratio = 0.2 and T = 280ºC. Water-gas shift catalyst weight adjusted between 0.01 and 0.1 to attain desired H_2:CO ratio.

The CO yield after the reformer increased from < 50% to 75% between 650°C and 1000°C, as shown in both Figure S-3 and Figure S-1 (d). Over the same range, the reformer product H_2:CO ratio decreased from 2 to 1.5 (Figure S-3 and Figure S-1 (f)). Thus, increasing the reformer temperature increases the CO yield but also increases the requirement on the water-gas shift unit.

Once the reformer product is fed through the water-gas shift unit in order to correct the H_2:CO ratio (to between 2 and 2.4), the shape of the overall CO yield curve changes to a parabolic-type trend. At high temperatures, whilst the reformer has a high CO yield, the H_2:CO ratio is so low that, in shifting it, the CO yield decreases significantly. An optimal CO yield for the syngas generation system was found at a reformer temperature between 750°C and 800°C.

Cold condensate

The first separation of Fischer-Tropsch products is done at 20 bar and 220°C in the Fischer-Tropsch reactor itself, where a liquid stream and vapour stream leave the reactor. The cold condensate, thereafter, is separated off from the light gasses (CH_4, CO, CO_2, H_2, N_2, C_2-C_{10}) in the vapour stream. Figures S-4 (a) and (b) show the effect of the cold condensate temperature and pressure on the amount and distribution of products (C_2-C_{40}) recovered in the liquid phase. For

Figure S-4 (a), the pressure is constant at 19 bar, whilst for Figure S-4 (b), the temperature is kept constant at 50°C. The arrow indicates the change that is required from Fischer-Tropsch conditions. The hydrocarbon distribution of the Fischer-Tropsch synthesis products is shown in both cases (red dotted line).

At temperatures close to Fischer-Tropsch conditions (200°C), the flash was relatively inefficient in ensuring high yields of distillate (C_{10}-C_{22}) in the liquid product. Instead, only C_{22+} remained as a liquid. Decreasing the temperature increased the total flow of liquid product and the yield of distillate which will be fed into the atmospheric distillation column. The temperature needed to be lowered quite substantially to minimize losses to the tail gas. A temperature of approximately 50°C appeared to maximize distillate yield, with only minor losses of C_{10}. Lower temperatures may have improved yield slightly more. However, this would require an enhanced cooling system for the downstream water knock out (limited to 35°C with cooling water).

By decreasing the pressure from 19 bar to 1 bar (Fig. S-5 (b)), the amount of distillate in the liquid phase decreased, and a significant portion of C_{10}-C_{15} was lost. Thus, maintaining as high a pressure and as low a temperature as possible ensures the best distillate yield.

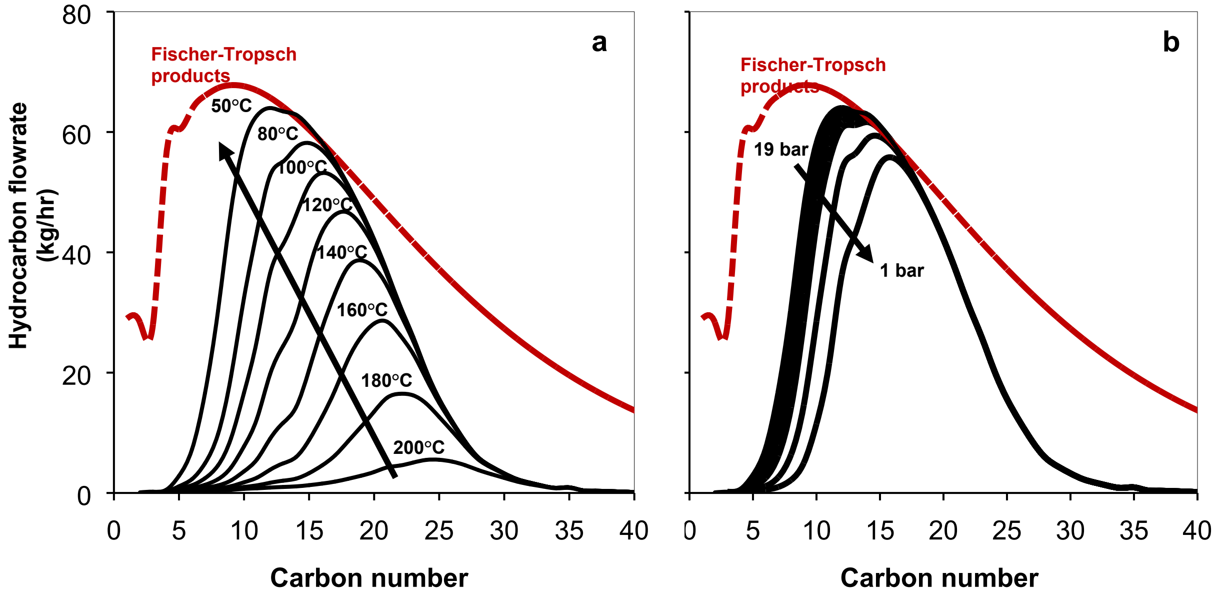

Figure S-4: Sensitivity analysis of the cold condensate flash showing the effect of (a) temperature at 19 bar and (b) pressure at 50°C on the product distribution recovered as liquid cold condensate from the vapour stream leaving the Fischer-Tropsch reactor.

Pre-hydrocracker flash

The Fischer-Tropsch liquid wax product contains small amounts of distillate (increasing with conversion), which can be over-cracked in the hydrocracker. Thus, depending on the composition of the Fischer-Tropsch wax, a pre-hydrocracker flash may be needed to separate off distillate from wax before it enters the hydrocracker. Figure S-5 (a) and (b) show the effect of the temperature (at 1 bar) and pressure (at 370°C) of the pre-hydrocracker flash on the product distribution of liquid wax entering the hydrocracker for a Fischer-Tropsch system operated at X_{CO}=60%.

By increasing the temperature, and decreasing the pressure, more distillate could be removed via the gas phase, thus avoiding over-cracking in the hydrocracker. However, at this Fischer-Tropsch conversion (X_{CO} = 60%) very extreme conditions (425°C and 1 bar) were required to separate off most of the distillate at the expense of heavier wax fractions that could be converted in the hydrocracker. Temperatures as high as 425°C would likely result in the thermal cracking of hydrocarbons. Thus, at a Fischer-Tropsch conversion of X_{CO} = 60%, the pre-hydrocracker flash does not appear to be practical. At higher Fischer-Tropsch conversions, the Fischer-Tropsch product distribution tends towards lighter products, thus the flash, operating at a lower temperature, may be useful to improve overall distillate yield.

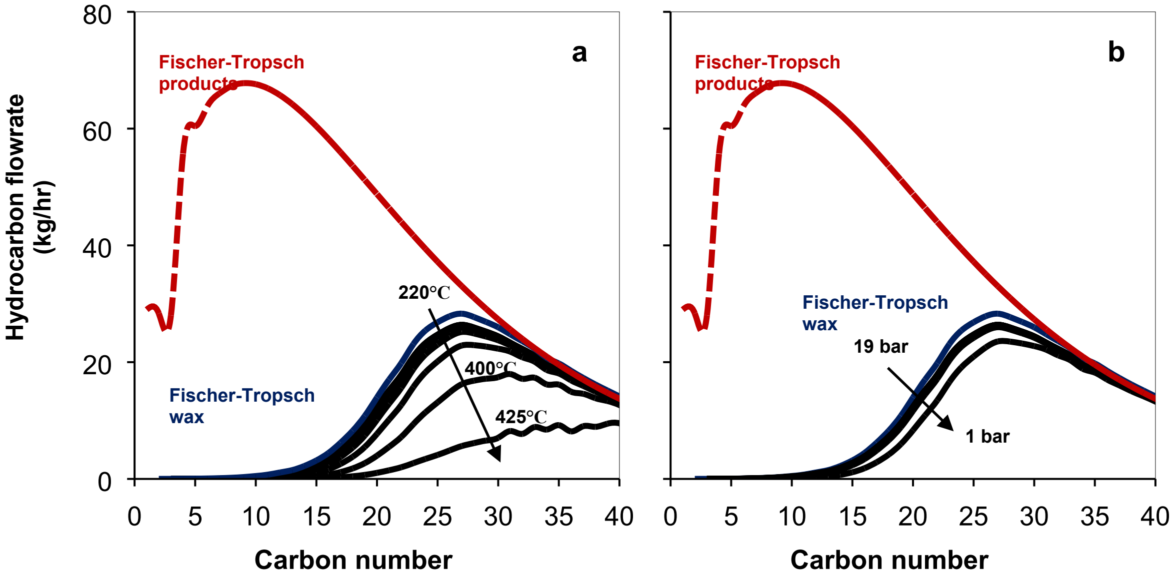

Figure S-5: Sensitivity analysis of the pre-hydrocracker flash showing the Fischer-Tropsch products (--), the Fischer-Tropsch wax products (--) and the resulting liquid products of the pre-hydrocracker flash (-) at different (a) temperatures at 1 bar and (b) pressures at 370°C.

By increasing the temperature, and decreasing the pressure, more distillate could be removed via the gas phase, thus avoiding over-cracking in the hydrocracker. However, at this Fischer-Tropsch conversion (X_{CO} = 60%) very extreme conditions (425°C and 1 bar) were required to separate off most of the distillate at the expense of heavier wax fractions that could be converted in the hydrocracker. Temperatures as high as 425°C would likely result in the thermal cracking of hydrocarbons. Thus, at a Fischer-Tropsch conversion of X_{CO} = 60%, the pre-hydrocracker flash does not appear to be practical. At higher Fischer-Tropsch conversions, the Fischer-Tropsch product distribution tends towards lighter products, thus the flash, operating at a lower temperature, may be useful to improve overall distillate yield.

Atmospheric distillation

The atmospheric distillation column is central to the separation and refining section. To minimize the equipment in this plant, a single distillation column was utilized with the distillate being pulled out as a side stream as shown in Figure S-6. The column was designed with 8 stages. The feed was fed to the column on stage 2 whilst the distillate side stream was pulled off from stage 7. These column specifications were based on the sensitivity analysis presented below.

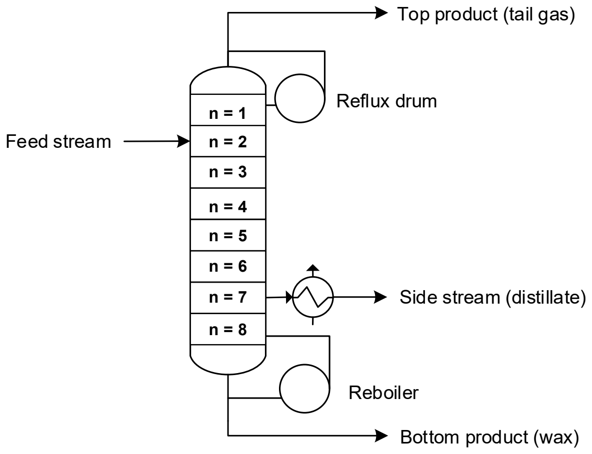

Figure S-6: Atmospheric distillation column showing the number of stages as well as the feed stage and the side stream product stage -based on the sensitivity analysis

Column specifications

Figure S-7 shows the effect of changing the (a) number of column stages 'n', (b) the feed stage and (c) distillate product stage on the hydrocarbon distribution of the distillate. This analysis was conducted for a column feed as shown in the base case stream table and a distillate side stream flow rate of 2 kmol/hr.

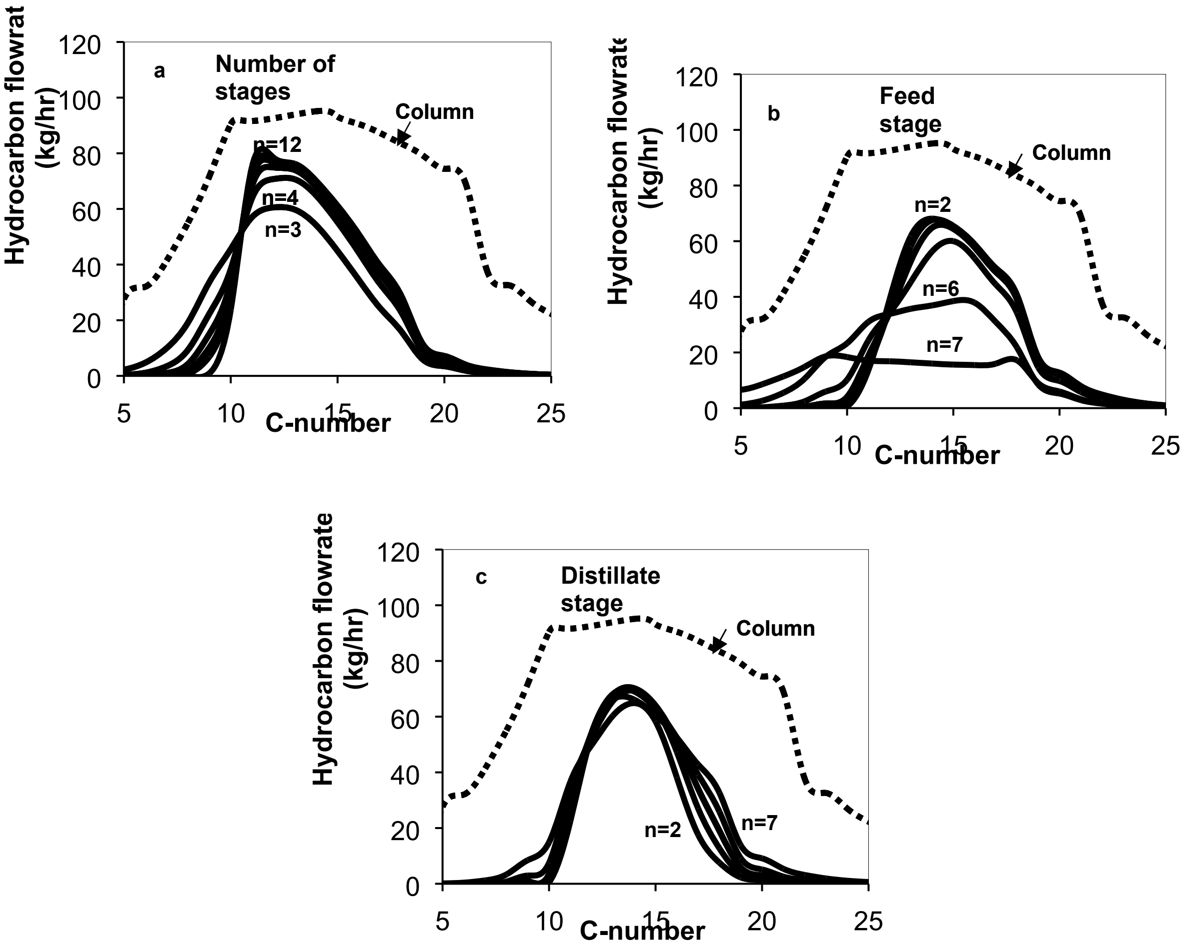

Figure S-7: The effect of the (a) number of column stages 'n', (b) feed stage and (c) distillate stage on the hydrocarbon distribution of the distillate side stream for a distillate flow rate of 2 kmol/hr with (a) feed stage = 2, distillate stage = n-1; (b) number of stages = 8, distillate stage = 7; (c) number of stages = 8, feed stage = 2.

Figure S-7 (a) shows the effect of the number of column stages on the hydrocarbon distribution of the distillate product for a column where the feed is fed in at stage 2 and the distillate leaves the column at stage n-1. Increasing the number of stages from 3 to 6 decreased the width of the distribution significantly whilst increasing the flow of hydrocarbons within the desired range of C_{10}-C_{22}. Increasing the column from 6 to 8 stages had a minor effect, narrowing the distribution slightly. Above 8 stages, there is an insignificant effect. An 8 staged column was thus chosen as the basis for the sensitivity analysis.

Figure S-7 (b) shows the effect of the choice of feed stage on the distillate product distribution for an 8 staged column with a side distillate stream at stage 7. A feed stage of 2, close to the top of the column resulted in a narrow distribution with maximum C_{10}-C_{22}. Moving the feed stage towards the bottoms widened the distribution into the lighter hydrocarbon range. This would negatively affect the distillate yield and, thus, for the sensitivity analysis in Section 10.3.7, a feed stage of 2 was chosen.

Figure S-7 (c) shows the effect of the distillate product (side stream) stage for a column with 8 stages with the feed fed in at stage 2. Operating with the distillate side stream at stage 2 resulted in a lighter product, with the hydrocarbon distribution shifted towards C_5-C_9. Increasing the distillate side stream stage resulted in a shift towards heavier hydrocarbons, albeit, not far out of the range of C_{10}-C_{22}. As increasing the flowrate of the side stream (to maximize yield) increases the number of light hydrocarbons in the distillate, it is important to maximize the number of hydrocarbons in the heavier distillate range by operating with a distillate stream at the lowest possible stage. Thus, for the sensitivity analysis, the distillate side stream was placed at stage 7.

Optimizing column specifications

The main objective of the distillation column is to maximize the overall carbon yield of distillate, whilst producing a distillate that meets the regional specifications of diesel (see Table S-5). The amount of product drawn out of the side stream, whilst maintaining the column within its operation limits, determines the distillate yield. However, the yield is limited by two distillate specifications: the flash point temperature limit, controlled by the number of light hydrocarbons, and the upper distillation temperatures (T_{90} and T_{95}), controlled by the number of heavy hydrocarbons.

This means that the distillation column conditions need to be optimized to maximize distillate side stream flow whilst also trying to minimize the fraction of light and heavy hydrocarbons. Figure S-8 shows the effect of the (a) distillate side stream flowrate, (b) column feed temperature, (c) reboiler duty and (d) reflux ratio on the distribution of distillate in the side stream. The column feed (···) is also shown, based on the base case scenario.

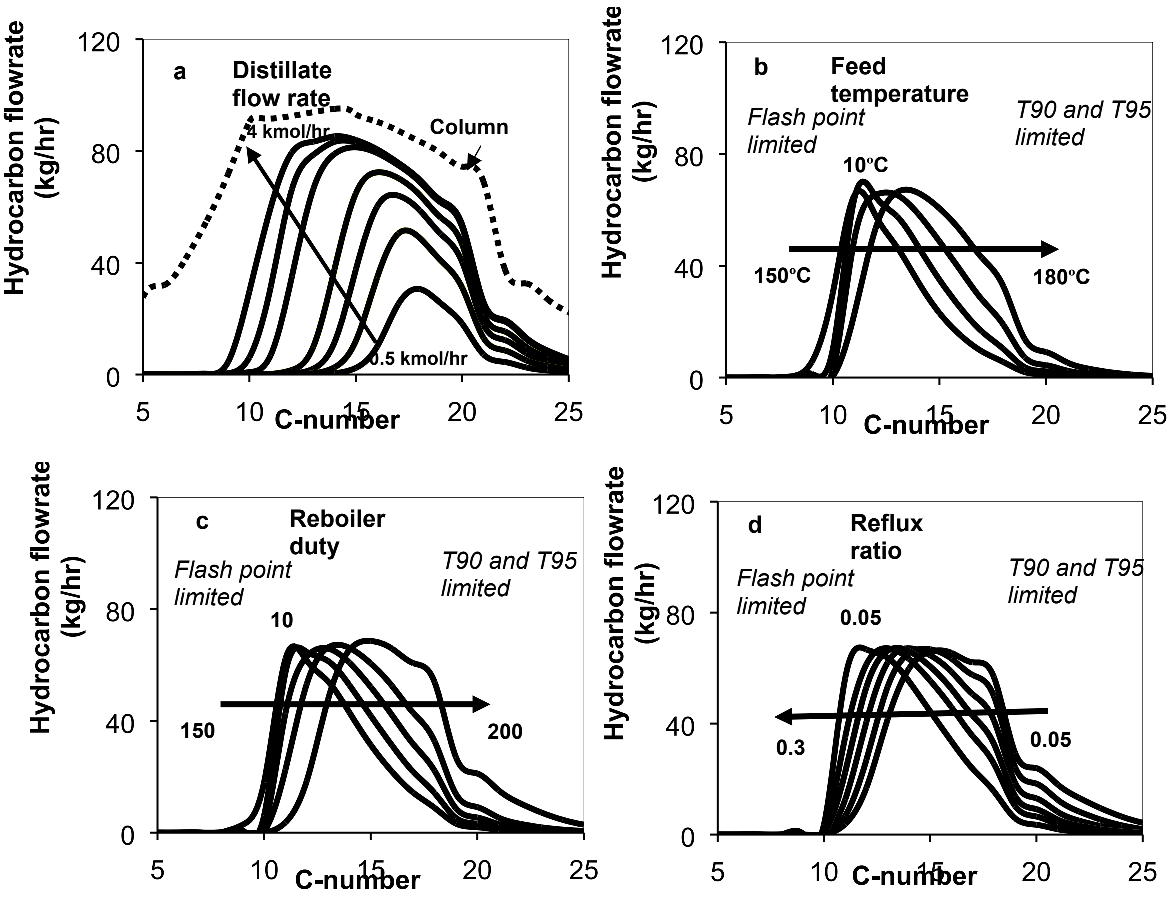

Figure S-8: Sensitivity analysis of the atmospheric distillation column showing the change in the side stream distillate hydrocarbon distribution as a function of (a) side stream flow rate, (b) inlet temperature, (c) reboiler duty and (d) reflux ratio.

Figure S-8 (a) shows the effect of increasing the flow rate of the distillate pulled off the side stream on the hydrocarbon distribution of that stream for a column feed temperature of 180°C, a reflux ratio of 0.2 and a reboiler duty of 180 kW. Increasing the distillate flow rate increased the size and width of the distillate hydrocarbon distribution, with a more significant effect towards the light range of hydrocarbons. The distillate side stream flow rate can be maximized by moving as close to the column feed distribution (···) as possible without breaching the flash point and T_{90} T_{95} limits.

In order to achieve this maximum, a certain level of flexibility is required to shift the distillate distribution towards the light and heavy range, so to stay within the region that satisfies both specifications. This flexibility may be achieved by adjusting the column feed temperature, reboiler duty or reflux ratio. The effect of the feed temperature on the resulting distillate distribution is shown in Figure S-8 (b), for a reboiler duty of 180 kW and a reflux ratio of 0.2. Increasing the inlet temperature shifted the product distribution towards higher carbon numbers, without significantly changing the shape of the distribution. The reboiler duty had a similar effect (Figure S-8 (c)). By increasing the reboiler duty from 150 kW to 200 kW (keeping the feed temperature constant at 180ºC and the reflux ratio at 0.2), the product distribution was shifted towards the heavier products. The reflux ratio had the opposite effect. Figure S-8 (d) shows the effect of increasing the reflux ratio from 0.05 to 0.3 at a constant feed temperature of 180ºC and a reboiler duty of 180 kW. By increasing the reflux ratio, the distribution was shifted towards lighter hydrocarbons.

Lower Fischer-Tropsch conversions (e.g. X_{CO} = 60%) result in a larger fraction of heavy hydrocarbons, thus lower feed temperatures, lower reboiler duties and/or higher reflux ratios may be required. Operating without a hydrocracker would also increase the fraction of heavy hydrocarbons in the column feed, thus requiring similar conditions.

Steam turbine

The only variables that could be adjusted on the turbine section were the feed rate of water to the boiler, the feed rate of air to the combustion unit, and the exit pressure of the pump. Since the feed rate of water was a manipulated variable in the control of the exit temperature of the boiler (set to 620ºC), only the latter two variables were used for sensitivity and optimization.

Figure S-9 shows the effect of the oxygen: feed (O:F) molar ratio on the power generated by the steam turbine. As the flow rate of air, and thus oxygen, was increased so too was the power generated by the steam turbine up to an O:F ratio of 0.32. This can be attributed to oxygen acting as a reactant in the exothermic combustion reaction. Oxygen increased the amount of energy produced in the exothermic reaction, which in turn increased the temperature of the gas leaving the combustion unit and thus the amount of heat that could be transferred to water to produce high pressure steam. As the amount of water was adjusted to ensure an exit temperature from the boiler of 620ºC; an increase in the temperature of the combustion gas resulted in more water that was turned into steam and thus a greater turbine output. Above an O:F ratio of 0.32 oxygen and nitrogen were simply acting as inert gasses, decreasing the temperature of the combustion

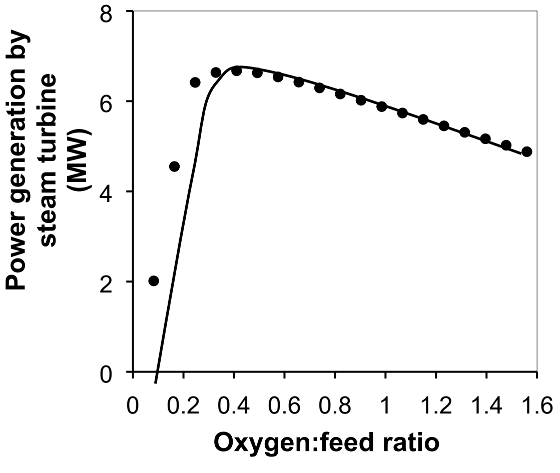

Figure S-9: Effect of the oxygen: feed ratio to the combustion unit on the power generation by the steam turbine at a pump exit pressure of 100 bar.

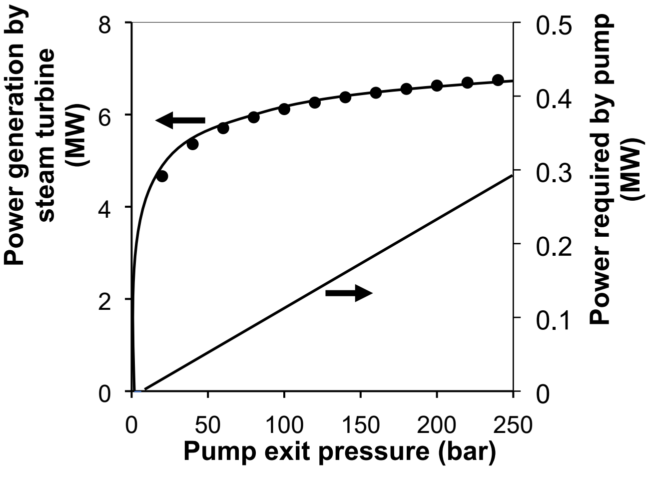

Figure S-10: Effect of pump exit pressure on power generation of the steam turbine (left axis) and power required for the pump (right axis) at an oxygen:feed ratio of 0.5.

products, and thus decreasing the power produced by the turbine. Thus, an O:F ratio of 0.32 appears to be an optimal feed ratio for power production.

Figure S-10 shows the effect of the water pump exit pressure on the power generated by the steam turbine. Steam turbines can typically operate at pressures from as low as 2 bar up to super critical steam pressures of 250 bar [58]. Increasing the pressure of pumped water increased the power generated by the steam turbine, albeit more significantly up to 60 bar (5.7 MW), after which the rate of improvement decreased slightly, with only 1 MW extra (6.7 MW) being generated between 60 bar and 250 bar. The power required to pump the water increases linearly between 0 MW and 0.3 MW within the range. Whilst this is not significant enough to create a maximum in terms of the net power production, operation above 100 bar appears to be the point at which the increase levels out and, thus, an optimal operating condition.

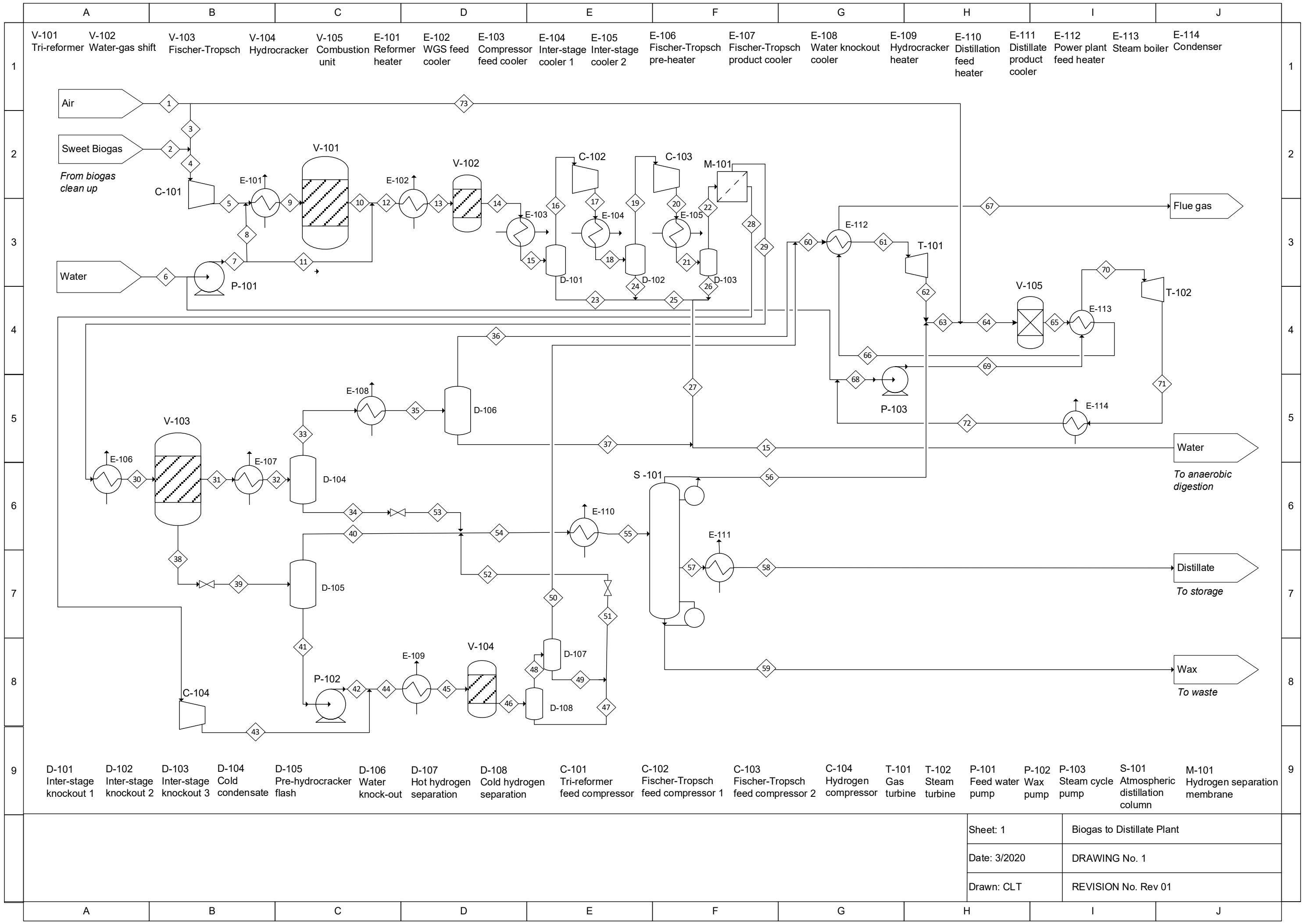

Figure S-11: Proposed once-through biogas-to-distillate Fischer-Tropsch plant